

Double-waveguide interband cascade laser with dual-wavelength emission

Robert Weih,¹ Julian Scheuermann,¹ Martin Kamp,² Johannes Koeth,¹ and Sven Höfling^{2,3}

¹ *Nanoplus GmbH, Oberer Kirschberg 4, Gerbrunn D-97218, Germany*

² *Technische Physik, Physikalisches Institut and Wilhelm Conrad Röntgen-Research Center for Complex Material Systems, Universität Würzburg, Am Hubland, Würzburg D-97074, Germany*

³ *SUPA, School of Physics and Astronomy, University of St Andrews, St Andrews, KY16 9SS, United Kingdom*

Abstract: Interband cascade lasers (ICLs) with dual wavelength emission have been realized by utilizing two spatially separated active regions in the same device. The two wavelengths (3.1 and 3.7 μm) were chosen in order to demonstrate that the usual spectral gain bandwidth of an ICL can be overcome. At 20°C, threshold current densities as low as 215 A/cm² (short wavelength) and 158 A/cm² (long wavelength) could be achieved in pulsed mode. It was possible for an epi-up mounted device to maintain dual-wavelength continuous-wave emission up to 0°C. Despite the longer wavelength emission being suppressed at higher temperatures, the shorter wavelength maintained an output power of more than 10 mW at 15°C.

Due to their low threshold power, interband cascade lasers (ICLs) [1] have evolved to competitive mid infrared (MIR) laser sources that can easily cover a wide spectral range since the transition energy can be varied independently from the bandgap of the materials used. ICLs, based on GaSb, have been shown to be operational at room temperature in continuous wave (cw) mode between 2.8 μm and 5.7 μm [2,3]. ICLs grown on InAs substrates have recently reached cw operation beyond 300 K at wavelengths around 4.7 μm [4]. Quantum cascade lasers (QCLs) utilize a similar concept wherein the emission wavelength is controlled by the layer thickness of the active quantum wells and hence the energy of the confined states. The fact that a QCL uses intersubband transitions results in a δ -function like density of transition states. Heterogeneous cascading can be made possible then by merging cascades with different emission wavelengths into one waveguide, while reabsorption can be avoided by appropriate design. This has been done in order to broaden the overall emission of the gain material [5] as well as to realize devices with dual wavelength emission [6,7]. The latter application has, additionally, been shown for ICLs, where two overlapping fundamental modes were demonstrated near 5 and 6 μm in pulsed operation, up to 235 K [8]. However, an unusual temperature dependence of the threshold current density was observed due to significant absorption of the lower wavelength photons via transitions from the higher wavelength lasing levels. This problem can be overcome by spatially separating the two active regions, as already shown for QCLs [9].

Here, we present a dual wavelength ICL with two spatially separated active regions designed for a short wavelength (SW) of 3.1 μm and a long wavelength (LW) of 3.7 μm . The emission wavelengths were adjusted via the thicknesses of the InAs layers of the W-quantum wells (W-QW). To maintain a similar electric field across all stages and hence be able to use a similar semi-metallic interface configuration in both active regions, the SW - electron injector contained the following six **InAs / AlSb** layer pairs: **4.2 nm / 1.2 nm; 3.1 nm / 1.2 nm; 2.5 nm / 1.2 nm; 2.0 nm / 1.2 nm; 1.58 nm / 1.2 nm; 1.58 nm / 2.5 nm**. The 5 InAs layers closest to

the W-QW were highly doped ($5 \times 10^{18} \text{ cm}^{-3}$) for carrier rebalancing. The LW - electron injector only contained five **InAs/AlSb** layer pairs: **4.3 nm / 1.2 nm**; **3.2 nm / 1.2 nm**; **2.45 nm / 1.2 nm**; **1.97 nm / 1.2 nm**; **1.97 nm / 2.5 nm** with the four InAs layers closest to the W-QW being highly doped ($5 \times 10^{18} \text{ cm}^{-3}$), again for carrier rebalancing.

Both active regions have their own GaSb separate confinement layers (SCLs) as indicated by the refractive index profile of the waveguide structure, represented by the dashed line in Fig 1. In order to compensate for the higher optical loss at longer wavelengths, so that both wavelengths would have similar threshold current densities, the LW active region comprised six stages while the SW active region comprised only four stages. In order to separate the two active regions and avoid absorption of the SW light in the LW active region, 2.5 μm of the short period InAs (2.43 nm) /AlSb (2.30 nm) superlattice was inserted between them. Due to the different active region designs and to account for the different optical mode distributions, the thicknesses of the SCLs were chosen to be 250 nm (SW) and 400 nm (LW). The calculated normalized profiles of the two modes are shown in Fig. 1 in blue (SW) and red (LW).

The epitaxial material was grown by molecular beam epitaxy on n-GaSb (100) substrates using an EIKO EV-100 system equipped with standard effusion cells for the group III elements and valved cracker cells for arsenic and antimony. The overall thickness of the structure adds up to more than 9 μm as can be seen in the scanning electron micrograph in the background of Fig. 1.

In order to extract the basic characteristics of the epitaxial material, 45 μm wide broad-area lasers were processed. After the definition of a BaF₂/Cr mask, an Ar/Cl₂ based dry etch proceeded through both active regions to avoid excessive current spreading and hence ensure a well-defined area for current injection. Afterwards, a Si₃N₄/SiO₂ passivation layer was deposited. Subsequently, a Ti/Pt/Au contact was evaporated on top. For smooth cleaving of the laser bars, the substrate was thinned to a thickness of 150 μm and a AuGe/Au contact was

evaporated on the back side and annealed at 250°C. After cleaving off 2.4 mm long bars, the lasers were electro-optically characterized in pulsed mode with a low duty cycle to avoid heating of the devices.

In Fig. 2. spectra of the broad-area lasers at 20, 40 and 60°C are shown. The corresponding drive currents were 320, 400 and 600 mA, respectively. Two well separated sets of Fabry-Pérot (FP) modes at 3.1 μm and 3.7 μm can be clearly seen over the entire temperature range indicating that both of the locally separated active regions are lasing. The envelope of the SW-modes shows a temperature shift of 1.7 nm/K, while the LW-envelope shifts with 1.84 nm/K. In Fig. 3, the temperature dependent threshold current density is shown for heat sink temperatures between 10°C and 80°C. They were determined by observing the appearance of the FP modes in FTIR spectra while increasing the drive current. At a temperature of 20°C, threshold current densities of 215 A/cm² (SW) and 158 A/cm² (LW) could be reached. To compensate for this difference, the number of cascades should be adjusted in the next iteration. From the exponential fit, the characteristic temperatures have been determined to be 46 K (SW) and 43 K (LW), which are comparable to literature values for ICLs [10].

Furthermore, lasers with a 5 μm layer of electroplated gold on top of the ridge for improved heat removal under cw operation were processed. In addition to the gold deposition, a highly reflective metal coating was applied to the back facet after cleaving. Otherwise, the sample was processed as specified before. In Fig. 4a.) the light-current-voltage characteristics at various heat sink temperatures are shown for a 1.2 mm long and 19.2 μm wide ridge which was soldered epi-up with PbSn on a copper heat sink. In the IV-curve of the device operated at a heat sink temperature of 0°C, a kink can be seen at 170 mA, which is the lasing threshold of the LW section. In Fig. 4b.) spectra are shown for various cw-current levels, indicating that the device is only operating in dual wavelength mode at higher injection currents. Clearly the SW section starts to lase at lower current levels even though its threshold current density was higher in pulsed mode, as shown in Fig. 3. The fact that the 1.2 mm long device shows dual wavelength

emission throughout all operating temperatures with similar thresholds for both wavelengths when being operated in pulsed mode implies that the behavior in cw mode is most probably of thermal origin indicating different heat removal from the two sections. At operating temperatures of 5°C and higher, no dual wavelength operation could be observed in cw mode. From the IV-curve at 20°C with only the SW section showing lasing, the set in voltage can be determined to be 4.4 V. This is 0.8 V more than the expected value of 3.6 V, estimated by taking into account the transition energies and the number of cascades in each active region. This additional voltage drop could originate from inadequate doping within the transitions between different waveguide sections. With a threshold voltage of 5.8 V and a threshold current of 100 mA, a threshold power of 580 mW can be calculated at an operating temperature of 20°C. The device emitted more than 10 mW of output power at a heat sink temperature of 15°C and was operational to at least 30°C in cw mode, which is suitable for a wide range of applications.

In summary, dual wavelength ICLs with two spatially separated active regions were designed and fabricated. The two emission wavelengths were 3.1 and 3.7 μm , which are in good agreement with the design values. From the emission spectra at different injection currents, the threshold current density could be measured independently to 215 A/cm² (SW) and 158 A/cm² (LW). Epi up mounted devices with an electroplated gold layer for improved heat dissipation could be operated in cw mode up to at least 30°C. However, above 0°C, only the emission from the SW cascade could be observed. In order to extend the temperature range for dual wavelength emission in cw mode, thermal aspects have to be taken into account in the future. Nevertheless, the concept of stacking more than one active region will make multi-wavelength devices without the limitation of the typical gain bandwidth feasible. With the introduction of an additional highly doped contact layer between the active regions and DFB processing routes, one can think of multi-port lasers which will enable gas absorption spectroscopy of multiple gases having absorption lines anywhere in the MIR region with a single device.

We are grateful for receiving financial support within the BMBF project “LASELO” (FKZ: 13N13773).

References

- [1] R.Q.Yang; Superlattices and Microstructures **17**, No.1, 77(1995).
- [2] J.Scheuermann, R.Weih, M.von Edlinger, L.Nähle, M.Fischer, J.Koeth, M.Kamp, S.Höfling, Applied Physics Letters **106**, 161103 (2015).
- [3] W.W.Bewley, C.L.Canedy, C.S.Kim, M.Kim, C.D.Merritt, J.Abell, I.Vurgaftman, and J.R.Meyer; Optics Express, **20** No.3, 3235 (2012).
- [4] L.Li, Y.Jiang, H.Ye, R.Q.Yang, T.D.Mishima, M.B.Santos, M.B.Johnson; Applied Physics Letters **106**, 251102 (2015).
- [5] C.Gmachl, D.L.Sivco, R.Colombelli, F.Capasso, and A.Y.Cho; Nature, **415** (2002).
- [6] K.J.Franz, K.T.Shui, S.R.Forrest, and C. Gmachl; International Conference on Indium Phosphide and Related Materials Conference Proceedings, 2006, pp. 26-29.
- [7] C.Gmachl, D.L.Sivco, J.N.Baillargeon, A.L.Hutchinson, F.Capasso, and A.Y.Cho; Applied Physics Letters **79**, 572 (2001).
- [8] L.Li, L.Zhao, Y.Jiang, R.Q.Yang, J.C.Keay, T.D.Mishima, M.B.Santos, M.B.Johnson; Applied Physics Letters **101**, 171118 (2012).
- [9] R.Blanchard, C.Grezes, S.Menzel, C.Pflügl, L.Diehl, Y.Huang, J.-H.Ryou, R.D.Dupuis, and F.Capasso; Applied Physics Letters **100**, 033502 (2012).
- [10] I.Vurgaftman, R.Weih, M.Kamp, J.R.Meyer, C.L.Canedy, C.S.Kim, M.Kim, W.W.Bewley, C.D.Merritt, J.Abell, and S.Höfling; J. Phys. D: Appl. Phys., **48**, 123001 (2015).

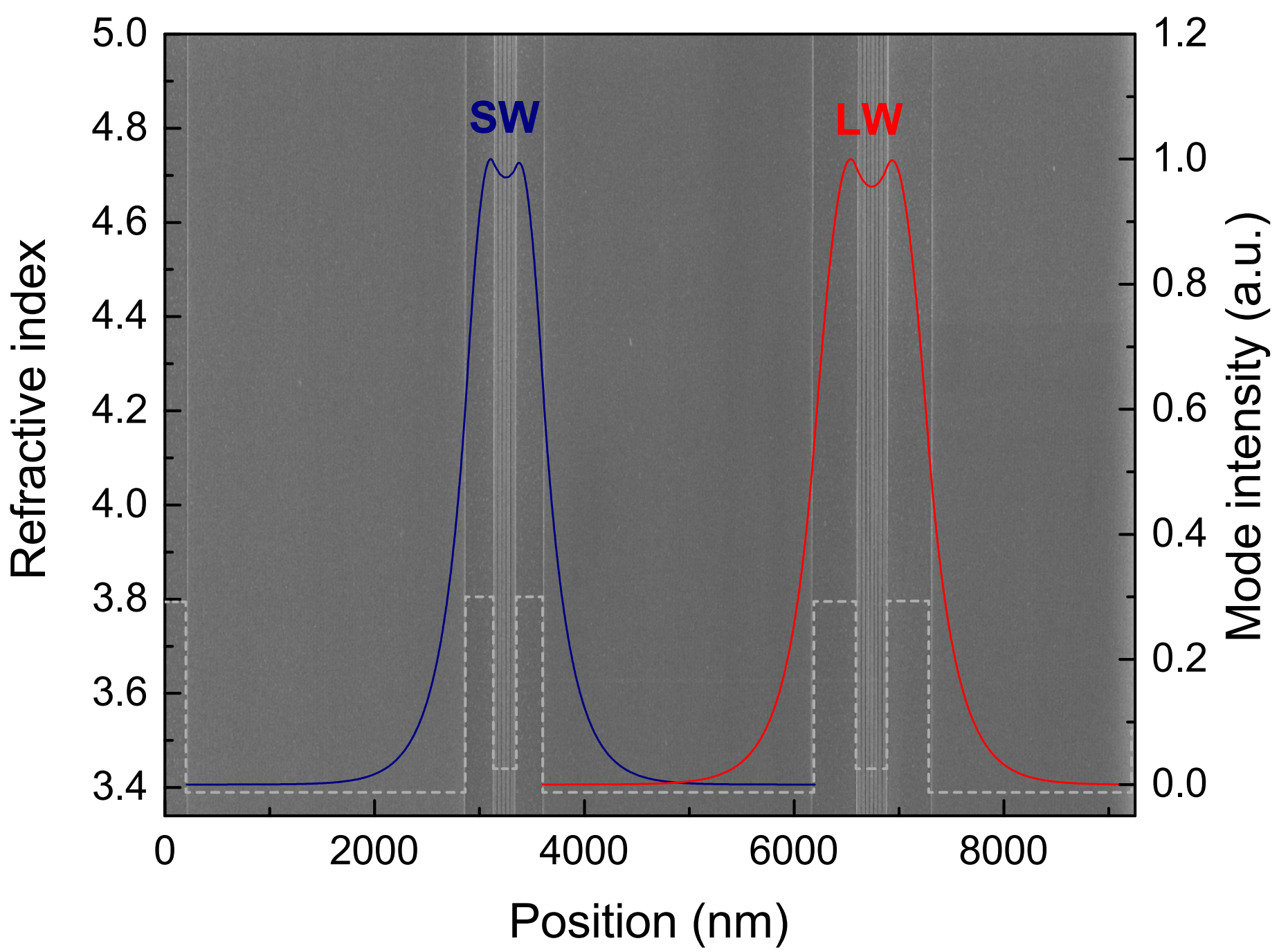
Figure Captions

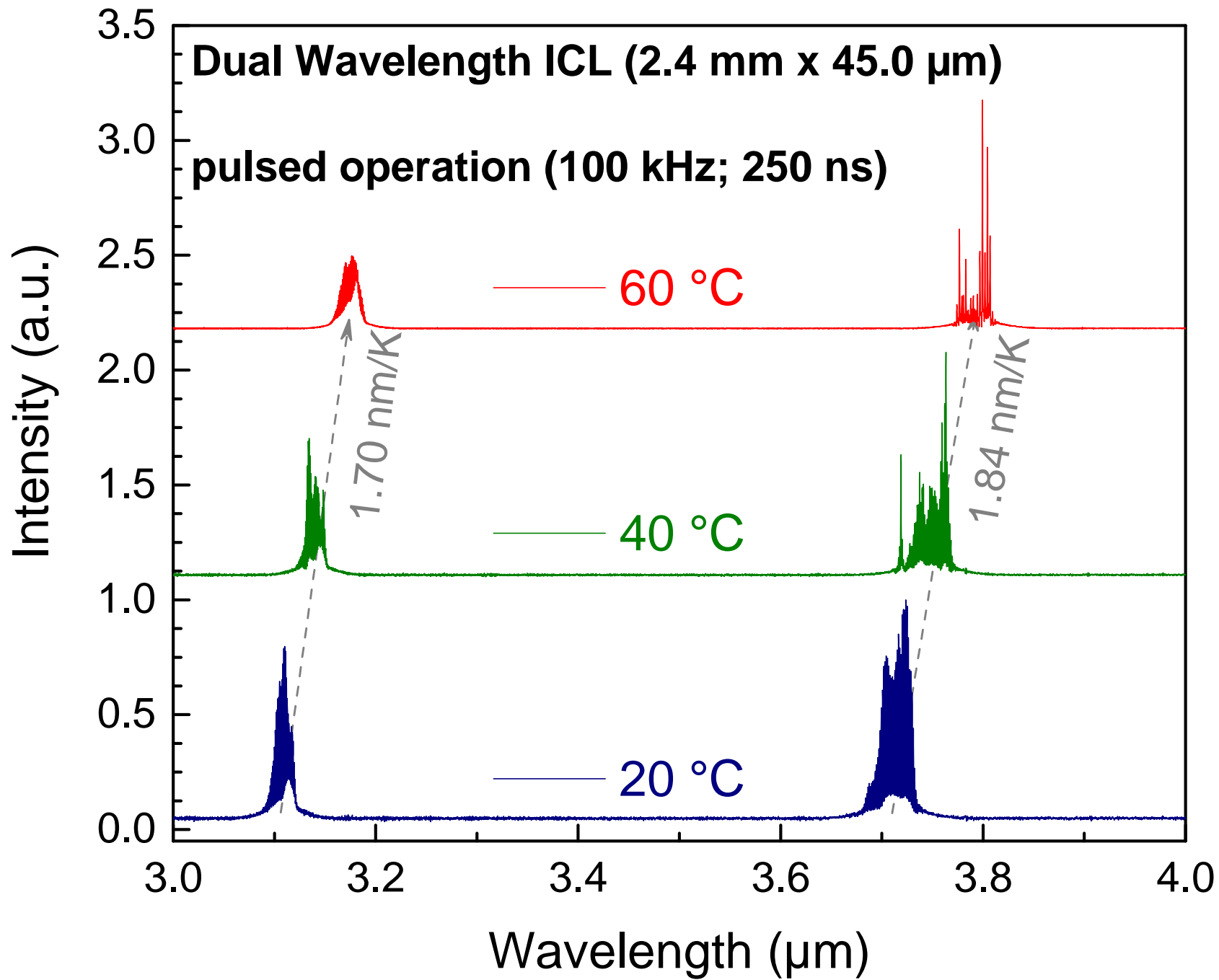
Fig. 1: Scanning electron micrograph from the cleaved edge of the epitaxially grown layer stack. The dashed line represents the refractive index of the different layers while the simulated optical mode distributions are displayed in blue (SW) and red (LW).

Fig. 2: Spectra of a dual wavelength ICL (2.4 mm x 45.0 μm) at different temperatures under pulsed excitation.

Fig. 3: Threshold current density of a dual wavelength ICL (2.4 mm x 45.0 μm) for both wavelengths in the temperature range from 10 to 80°C. The dashed lines represent the characteristic temperature exponential fit.

Fig. 4: (a) Light-current-voltage characteristics of an epi-up mounted dual wavelength ICL with electroplated gold and a highly reflective back facet operated in cw mode at several temperatures. (b) Spectra of the same device at a heat sink temperature of 0°C at different drive currents (device dimensions: 1.2 mm x 19.2 μm).





Dual Wavelength ICL (2.4 mm x 45.0 μm)

pulsed operation (1 kHz; 300 ns)

